V International Conference on Particle-based Methods – Fundamentals and Applications
PARTICLES 2017
P. Wriggers, M. Bischoff, E. Oñate, D.R.J. Owen, & T. Zohdi (Eds)

GRAY-SCALE LATTICE BOLTZMANN – AN ATTEMPT TO BRIDGE MULTIPLE LENGTH SCALES

GERALD G. PEREIRA[1] AND M. BEN CLENNELL[2]

[1]Computational Modelling, CSIRO
Private Bag 10, Clayton South, 3169, AUSTRALIA
Gerald.Pereira@csiro.au and www.csiro.au

[2]Energy, CSIRO
Bentley, 6098, AUSTRALIA
Ben.Clennell@csiro,au and www.csiro.au

Key words: Lattice Boltzmann, porous media, heterogeneous, multiphase, convection.
Abstract. Understanding and controlling the flow of fluids through porous media such as rocks, fibres, granular media and paper is of fundamental significance to a variety of industries such as oil and gas, chemical production, health and sanitary products. Numerical modelling of this physical process can be difficult not only because of the complex, three-dimensional topology of the porous medium but also because of computational limitations. For example, shale rocks which is now being intensively investigated for its oil and gas resources have porosity over a wide range of length scales from nano-metres up to millimetres. It has been shown that the micro-porosity is fundamental to the fluid movement through the rock. However, current numerical models, which work off computed tomographical (CT) scans of the rock will be excessively large if they are to fully model all length scales which may span six or more orders of magnitude.

Here we consider the development of a lattice Boltzmann (LB) technique which may be able to solve the fluid flow over a wide range of length scales. In the past LB techniques have proven to be ideal to model fluid flow in complex porous media since it can readily import and process digital data from CT scans. Hence the fluid flow field is quickly determined and permeabilities can be predicted. However, when the CT data contains micro-porosity, the conventional LB method is not applicable and a modified LB method needs to be developed. Here we consider a gray-scale LB method which works on voxels which are not fully void or solid but something in between, i.e. each voxel is partially resistant to fluid flow. We firstly outline the model, then validate it on test cases and then demonstrate its applicability on real porous media.

We develop models not only for single phase fluid flow, but also multiphase fluid flow (i.e. a gas and a liquid) as well as a temperature model, where the temperature field is advected by the fluid flow. For all these cases the models are developed and validated and then demonstrated on realistic media. It is shown that the gray-scale LB model may be able to solve for fluid flow through multiple length scales – a difficult computational problem which is of increasing significance in many real-world applications.

1 INTRODUCTION

The lattice Boltzmann (LB) method is a fluid particle based numerical method which considers the Boltzmann transport equation as the basis for fluid motion. The lattice Boltzmann solution is restricted to discrete lattice sites (nodes) but has proven to be a powerful alternative to solving the Navier-Stokes equations, especially for problems with complex boundaries [1, 2] such as those found in porous media.

In the past the LB method has been successfully to solve for fluid flow through rocks, such as sandstone, carbonates and shales or fibrous materials such as paper products. In these cases if a digital image of the sample (i.e. a computed tomo-graphical or CT scan) is available, the LB method may be applied to this image to obtain the fluid flow through the sample. Conventionally, each voxel of the digital image corresponds to a region of solid material (i.e. not available for fluid flow) or pore space (i.e. void region which is available for fluid flow) and the LB method solves then on all the void voxels, with appropriate boundary conditions at the interface between solid and void. The fluid flow through the porous sample may be then determined. In this paper we refer to such a model as a black-white model as each voxel (lattice node) corresponds to either solid or fluid. Through a Chapman-Enskog expansion, the LB scheme has been shown to be equivalent to solving the Navier-Stokes equations for fluid flow [1, 2].

The gray-scale LB method attempts to lift the restriction that each lattice node is either fluid or solid. In this case, nodes can be anything between solid or void, i.e. a gray-scale value. Fluid can then flow through these gray lattice nodes, but there is an increased fluid resistance associated with this flow. The magnitude of this fluid resistance at a particular voxel will be related to the degree of gray shading of that voxel. Such a model should be useful in situations where the corresponding CT scan has a lower resolution than the fine-scale structure of the sample (i.e. the CT scan resolution may be of the order of microns, but the pore structure might be of the order of 10-100nm). Thus a specific voxel will contain both solid and void regions and would appear as a shade of gray in the CT image.

To develop a suitable gray-scale LB model it is useful to first outline the main steps for the conventional (black-white) LB solution. LB is a class of cellular automata, which is solved on a regular lattice (usually simple-cubic in three dimensions). On each lattice vertex or node, where the location of each node is the centre of a voxel from the CT scan, a set of fluid particle distribution functions is defined. There are Q distribution functions defined on each node. LB method then consists of three main steps. The first step is called streaming, in which all fluid packets (distributions) are moved to adjacent sites. This streaming can be correlated to the normal advection of fluid. The second step is called bounce back, which accounts for fluid-solid boundary conditions. Here fluid packets at boundary nodes are reversed in direction (or more complicated half-way bounce back or interpolation boundary conditions may be implemented). The final step in LB is a collision step where fluid packets converging on a given node are redistributed according to the Maxwell distribution. The LB method then consists of iterating these three steps (in a pseudo time-stepping manner) to give a solution. In the gray-scale model there are no fluid-solid boundaries, as such. All voxels are allowed a certain degree of flow. This can be related to the solid fraction in that voxel, but other effects such as tortuosity, topology, mineral content etc can be included into the model to contribute

to the voxel's resistance to flow. To account for this, a partial bounce-back rule is imposed on each voxel [3,4].

This means at each voxel a certain fraction of fluid packets (which were streamed into a node) will be bounced back. We denote the fraction of fluid packets, which are bounced back at a node by n_s ($0 \leq n_s \leq 1$) and each node can have a different n_s value.

At important question in the implementation of a suitable gray-scale LB model is how does one estimate the bounce-back fractions n_s from a gray-scale CT sample? As a first-step towards doing this, we estimate this by using the partial volume fractions of materials and pores which are generated through a data-constrained modelling (DCM) approach [5]. In this method each voxel is represented by partial volumes of various different materials rather than the binary value of only one material present in the traditional image segmentation. The DCM methodology has been applied to a number of other systems successfully. It is important to emphasize that n_s may have a number of other contributions, rather than just partial volume fractions of different materials, e.g. fine-scale topology, tortuosity and anisotropy.

In this paper we present a gray-scale model for single phase fluid flow through a digital image of porous media where each voxel (which makes up the digital image) imparts a certain resistivity to fluid flow. We only use a single-relaxation time (SRT) in this paper, although the gray-scale can be readily applied to multiple relaxation time schemes. After validating the model, we apply it to real-world rock samples. We then show how the gray-scale LB model can be extended to multiphase, immiscible flow and again validate the model against test cases, before applying it to some more realistic samples. Finally we couple the gray-scale fluid flow model to heat transfer, where the heat may be convected via the fluid or heat may naturally diffuse through the fluid. The heat transfer model is once again validated against test cases before application to an actual rock sample.

2 GRAY-SCALE LB

The LB model is a mesoscopic numerical method used to study incompressible fluid dynamics. Its main advantages over more conventional CFD techniques (which directly solve the Navier-Stokes equations) are its programming simplicity, computational efficiency and inherent parallelism due to a large amount of local computations. In addition, as mentioned in the Introduction, it naturally deals with complex porous media if suitable digital information is provided. Details of this method, applied to single phase flow, are available [1,2] and thus we shall only focus here on the LB method applied to gray-scale models.

As explained in the Introduction, LB consists of streaming, collision and bounce-back at boundaries. More complex and accurate boundary conditions such as half-way bounce-back or linear interpolation boundary conditions are also possible. In the collision step particle distributions relax towards a given equilibrium distribution - a Maxwellian distribution. Then macroscopic properties such as fluid density, fluid velocity and the stress tensor can be derived from the particle distributions. If we are dealing with only a single fluid, one set of particle distributions is defined, i.e. $f(\boldsymbol{r}, \boldsymbol{u}, t)$ which denotes the distribution of particles travelling with a particular velocity $\boldsymbol{u}$ at time t at lattice node $\boldsymbol{r}$. We will only consider a three dimensional (3D) model in this paper so that we implement the common D3Q19 model which indicates that there are 18 possible vectors, $\boldsymbol{e}_i$, in which particles may move in addition to the

null vector. These 18 possibilities are the vectors (±1, 0, 0), (0,±1,0), (0,0,±1), (±1,±1,0), (±1,0,±1), (0,±1,±1).

We solve the following LB equation at every node for the distribution function with velocity e_i:

$$f_i(\boldsymbol{r}+\boldsymbol{e}_i\Delta t, t+\Delta t) - f_i(\boldsymbol{r},t) = -\frac{1}{\tau}\left[f_i(\boldsymbol{r},t) - f_i^{eq}(\boldsymbol{r},t)\right]. \quad (1)$$

The term f_i^{eq} is the equilibrium Maxwell distribution given by

$$f_i = w_i\rho\left[1+\frac{\boldsymbol{e}_i\bullet\boldsymbol{u}^{eq}}{c_s^2}+\frac{(\boldsymbol{e}_i\bullet\boldsymbol{u}^{eq})^2}{2c_s^4}-\frac{\boldsymbol{u}^{eq}\bullet\boldsymbol{u}^{eq}}{2c_s^2}\right], \quad (2)$$

where w_i are weights which are defined for the given D3Q19 model. In Eq.(1), τ represents a relaxation time and it can be shown to be related to kinematic viscosity via $\nu = c_s^2(\tau - 1/2)$ where c_s is the sound speed and c_s^2 equals 1/3. The pressure, P, in this model is given by the equation of state $P = c_s^2\rho$. The LB equation (1) is known in the literature as single relaxation time (SRT) scheme, because only one relaxation time is involved.

The relationship to macroscopic parameters such as density and velocity are given by

$$\rho = \sum_i f_i \quad and \quad \rho\boldsymbol{u} = \sum_i f_i\boldsymbol{e}_i. \quad (3)$$

To model forces (such as body forces to mimic gravity or even surface forces between different phases when we model two or more phases) we add an explicit forcing term to the LB equation (1). This forcing term is defined by

$$\Im_i = \frac{F\bullet(\boldsymbol{e}_i-\boldsymbol{u}^{eq})}{\rho c_s^2}f_i^{eq}, \quad (4)$$

where $\boldsymbol{F}$ is the force. The macroscopic velocities are modified in this case to $\rho\boldsymbol{u} = \sum_i f_i\boldsymbol{e}_i + \boldsymbol{F}/2$ and $\boldsymbol{u}^{eq} = \boldsymbol{u}$. This implementation of an applied force is not only accurate, but also exhibits correct time evolution of the flow.

Typically LB methods solve on (100%) void nodes and don't solve on solid nodes. To simulate no-slip boundary conditions, at boundaries between void and solid nodes, a bounce-back step is performed which simply reverses the direction of the streamed distribution function. In the gray LB methods, one solves at *all* nodes. Since there are no solid nodes, as such, a full bounce back is not performed. Rather, on any given node a certain fraction of the fluid packets that are streamed into that node are bounced back. This fraction of fluid packets which are bounced back at any given node is given by n_s and so equation (1) is replaced by

$$f_i(\boldsymbol{r}+\boldsymbol{e}_i\Delta t, t+\Delta t) = (1-n_s)f_i(\boldsymbol{r},t) - \frac{1}{\tau}(1-n_s)\left[f_i(\boldsymbol{r},t) - f_i^{eq}(\boldsymbol{r},t)\right] + (1-n_s)\Im_i + n_s\,\hat{f}_i(\boldsymbol{r},t). \quad (5)$$

The last term with the circumflex on the distribution function indicates the distribution function to be added is in the opposite direction to i. The parameter n_s is between 0 and 1, and can be related to voxel compositional and/or topological properties (among other things). The macroscopic velocity is now

$$\rho\boldsymbol{u} = (1-n_s)\left(\sum_i f_i\boldsymbol{e}_i + \boldsymbol{F}/2\right). \quad (6)$$

Equation 5 represents the gray-scale LB model of Walsh et al [3]. This gray-scale LB model was validated against the Brinkman extended Darcy model with the flow field equation

given by

$$\nabla^2 u - \left(\frac{\phi}{\nu}\right) u = \frac{1}{\rho\nu} G \qquad (7)$$

where G is a driving force or pressure gradient, u is the velocity field, ν is the kinematic viscosity, ρ fluid density and ϕ is a damping coefficient. Equation 7 is the Brinkman extended Darcy equation where ϕ is related to n_s via $\phi = 2n_s$ [3]. When $\phi \to 0$, the solution to (7) returns to the standard Poiseuille equation. It can be solved analytically with solution expressed as

$$u(y) = -\frac{G}{\phi\rho}\left[1 - \frac{\cosh[r(y - L/2)]}{\cosh(r \cdot L/2)}\right] \quad , \qquad (8)$$

where ϕ and r are related via $r = (\phi/\nu)^{1/2}$.

Solutions for various n_s values are shown in Fig, 1 and we also show the corresponding permeability as a function of n_s. Excellent agreement is found between the analytic and LB gray-scale method. Further comparisons for layered channels (i.e. variable n_s) between the LB gray-scale model and analytic solution also show excellent agreement [4].

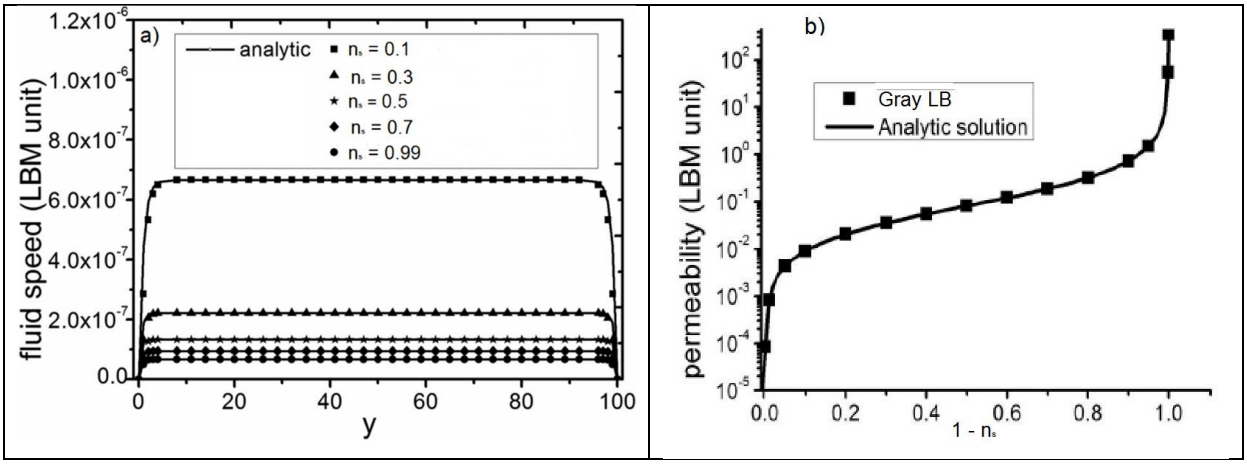

Figure 1a) Comparison between analytic solution (black curves) and LB gray-scale model for various n_s values for a) velocity field and b) effective permeability for Brinkman flow in a 3D channel .

3 MULTIPHASE FLOW

Figure 1 gives us some confidence in the single phase gray-scale LB model so that we now proceed to applying an extension of it to two (or more) immiscible phases. In principle there can be n phases. To model this with our LB method we now define n sets of distributions functions, which represent each immiscible phase - $f^1(\mathbf{r},\mathbf{u},t)$ ... $f^n(\mathbf{r},\mathbf{u},t)$. For each phase we solve the LB equation at node i. So for the k^{th} phase (where $k \in 1,...n$) we need to solve the LB equation (1), with k (possibly different) relaxation times. Values for various macroscopic variables in this model then follow almost analogously to the single phase equations for density, viscosity and momentum flux for each phase.

To model immiscibility between phases we implement the *pseudo-potential* model [6] which employs nearest neighbour inter-particle potentials to model the interactions between

components. In a sense this follows physical reality at the microscopic level where molecules interact via short-range Lennard-Jones type potentials. In the original Shan-Chen [7] model lattice nodes which have a separation of less than or equal to $2^{1/2}$ units are coupled together. The interaction potential between components is accommodated via a force, F^k which is introduced through the added force term (Eq. (4)). The equilibrium velocity is re-defined to accommodate multiple phases, i.e., $\boldsymbol{u}_k^{eq} = \boldsymbol{u}'$. Here $\boldsymbol{u}'$ is a combined velocity and to satisfy momentum conservation must be

$$\boldsymbol{u}' = \frac{\sum_k \tau_k^{-1} \rho_k \boldsymbol{u}_k}{\sum_k \tau_k^{-1} \rho_k} \quad . \qquad (9)$$

The fluid-fluid interaction for phase k at lattice node $\boldsymbol{r}$ is then given by

$$\boldsymbol{F}^k(\boldsymbol{r}) = \rho_k(\boldsymbol{r}) \sum_{k \neq k'} g_{kk'} \sum_i w(|\boldsymbol{e}_i|^2) \rho_{k'}(\boldsymbol{r} + \boldsymbol{e}_i) \boldsymbol{e}_i \ , \qquad (10)$$

where $g_{kk'}$ is the interaction potential (or coupling parameter) between dissimilar components. The weights w depend on the separation between interacting nodes with $w(1)=1/6$ and $w(2)=1/12$. Note, we assume the coupling is zero for similar components. The pressure in this model is given by the equation of state

$$P = c_s^2 \sum_k \rho_k + \frac{1}{2} \sum_{kk'} g_{kk'} \rho_k \rho_{k'} \ . \qquad (11)$$

One of the issues with this nearest neighbour implementation is that it leads to large spurious currents which are a numerical artefact. These numerical artefacts, if not reduced to a minimum, will lead to large numerical instabilities. Thus we shall attempt to reduce these numerical instabilities. It has been found extending the range of the pseudo-potential leads to a significant reduction (up to 1000 times) of these spurious currents. The range of pseudo-potential can in principal go to infinity but this of course comes at a computational cost. We have implemented here both 6th order (including all neighbours less than or equal to 2 units away) and 8th order (including all neighbours less than or equal to $8^{1/2}$ units away) pseudo-potentials. This increases the number of neighbours to be sampled from 18 (Shan-Chen) to 32 (6^{th} order) to 64 (8^{th} order), but greatly enhances the numerical stability of the method. Weights, which are required in Eq. (9), for the additional neighbour pairs have been given previously.

The final step in the gray-scale, multiphase LB model is to incorporate the effect of voxel resistivity to flow. We assume the resistivity of a particular voxel can be different for different phases. Physically this may be the case if there are different materials in a voxel which have different slip conditions with different fluids. So equation (5) becomes:

$$f_i^k(\boldsymbol{r} + \boldsymbol{e}_i \Delta t, t + \Delta t) = (1 - n_s^k) f_i^k(\boldsymbol{r}, t) - \frac{1}{\tau_k}(1 - n_s^k)\left[f_i^k(\boldsymbol{r}, t) - f_i^{k,eq}(\boldsymbol{r}, t)\right] + (1 - n_s^k)\Im_i^k + n_s^k \hat{f}_i^k(\boldsymbol{r}, t). \qquad (12)$$

The macroscopic velocity for each phase is defined similarly to equation (6) with suitable n_s^k, f^k and $\boldsymbol{F}^k$ values used for each component.

For the simulations presented here we use $\tau_A = 1$, $\tau_B = 2.0$, which implies $\nu_A = 1/6$, $\nu_B = 1/2$, the mass of phase A is 1.0 while mass of phase B is 2.0. The surface tension g_{AB} between phases is 1.33. Note, that unless we use the numerically stable multiphase model described above, we would not be able to have a disparity in these values (between the phases) and such a large g_{AB} value.

We initially look at two-phase channel flow, i.e. phase 1 displacing phase 2 in a narrow channel (width 42 units, depth 22 units and length 152 units). We tried a range of n_s values to see how the flow changed. Figure 2 (which is a slice taken at the middle of the smallest dimension) shows the flow for n_s = 0.1 with a given body force of 6.8 x 10^{-3}. Note that we impose periodic boundary conditions in the direction parallel to the body force, i.e. any fluid exiting the domain through a face perpendicular to the body force vector re-enters on the opposite face. Other cases of n_s = 0.0, 0.05, 0.3, 0.5 and 0.7 were also simulated with the gray-scale LB method.

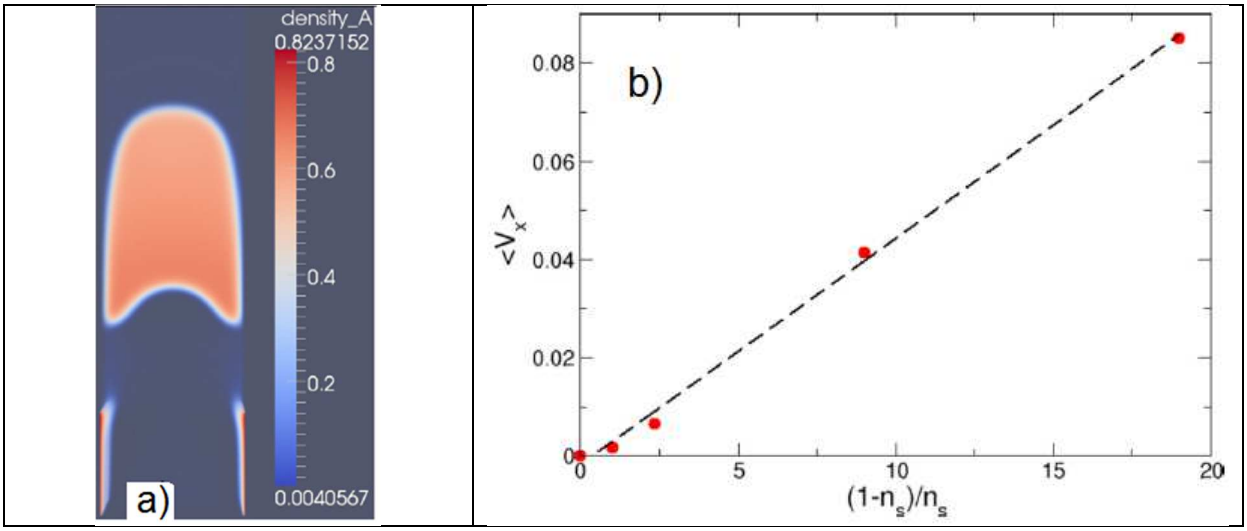

Figure 2. a) Two phase flow in a channel of width 41 units and depth 21 units for n_s = 0.1 after 2100 LB time-steps. The A-phase begins at the bottom of the channel. b) Plot of the average channel velocity of phase A versus $(1-n_s)/n_s$. Red circles come from gray-LB method while the dashed line is a best fit to these results with a gradient of 4.6×10^{-3}.This dashed line should be compared to Eq. 14.

The shape of the interfaces in Fig. 2 result from a combination of the surface tension, applied body force and applied n_s value. In Fig. 2a although the n_s value is 0.1, the comparatively large body force results in a large fluid velocity, which yields a curved (parabolic) interface profile. As the n_s value is increased, the interface becomes less curved and more flattened. A larger body force needs to be applied as the n_s value is increased because n_s is directly related to fluid drag.

According to Darcy's Law the average velocity in a porous medium is given by

$$\langle V_x \rangle = \frac{Gk}{\nu\rho} \quad . \qquad (13)$$

So the average velocity is proportional to the permeability, k. In the gray-scale models the permeability is related to n_s via $k = (1-n_s)\nu/2n_s$ [3], so that the average velocity along the channel is given by

$$\langle V_x \rangle = \frac{G(1-n_s)}{2n_s\rho} \quad . \qquad (14)$$

We can determine the average velocity quite easily in these simulations by tracking the location of the advancing interface (fluid front). Doing this for the four different simulations (at the same G value) and plotting the average velocity as a function of n_s gives Fig. 2b. Note, we have also added the $n_s = 1$ value which gives zero channel speed (see equation (6)). We obtain a linear relationship between the average channel velocity and $(1-n_s)/n_s$, as predicted by equation (14). Furthermore, from the gradient of the graph and assuming an average A-phase density of 0.75, we predict the body force is 6.9×10^{-3}, which agrees well with the body force we have applied in these cases.

Further test were also carried out to validate the model [4] and demonstrated the model was accurate. One important note here is that to increase the numerical stability of this model it is desirable to use multiple relaxation time (MRT) scheme,

4 GRAY-SCALE LB WITH TEMPERATURE COUPLED TO FLOW

The temperature field is assumed to be only advected by the fluid flow. Viscous fluid heating is assumed to be insignificant and hence is neglected in this model. The model used for the temperature field calculation is the *passive-scalar* model and has been implemented before with a single-relaxation time LB model for binary (black-white) nodes [8]. The temperature field obeys the equation

$$\frac{\partial T}{\partial t} + (u \cdot \nabla)T = \nabla \cdot (\alpha \nabla T) + \psi \qquad (15)$$

where T is the temperature, u is the velocity field, α is the thermal diffusivity and ψ accounts for all (heat) source terms. This equation has a similar form to the momentum (Navier-Stokes) equation and so the same equilibrium distribution function (i.e. Eq. 2) that has already been used for the fluid density and velocity fields may be also used for the temperature. However a different relaxation time (in the collision operation, i.e. Eq. 5) is used. This relaxation time, which we denote as τ_α is related to the thermal diffusivity by $\alpha = c_s^2(\tau_\alpha - 1/2)$. The temperature is then given by the summation of probability distribution functions, with τ_α used in the collision process. Appropriate boundary conditions are used on the temperature field (at boundaries between solid and liquid) such as constant temperature and at inlets or outlets [9] .

To validate the gray-scale LB temperature model we again consider Brinkman flow solution for the fluid (Eq. 8) and couple this with temperature evolution equation (15). We consider the steady-state solution so that the time dependent term is zero. The solution depends on the Peclet number, Pe, which is defined ratio of advective transport to diffusive transport. We solve this partial differential equation in a channel with a uniform n_s value. The n_s value determines the magnitude of the fluid velocity which in turn determine the Peclet number. The partial differential equation is solved with a finite difference method and the solution is then compared to the corresponding gray-scale LB solution. Figure 3 shows comparison of the longitudinal (in the direction of the pressure gradient) and orthogonal

temperature profiles for a Peclet number of 0.194. The black circles correspond to the LB simulation solution while the red curve corresponds to the finite difference solution of the continuum partial differential equation. Excellent agreement is obtained between the two methods. Further validations have also been carried out for other Peclet values [9] which show a similar level agreement between LB and finite difference solution. This indicates the LB gray-scale method has good accuracy.

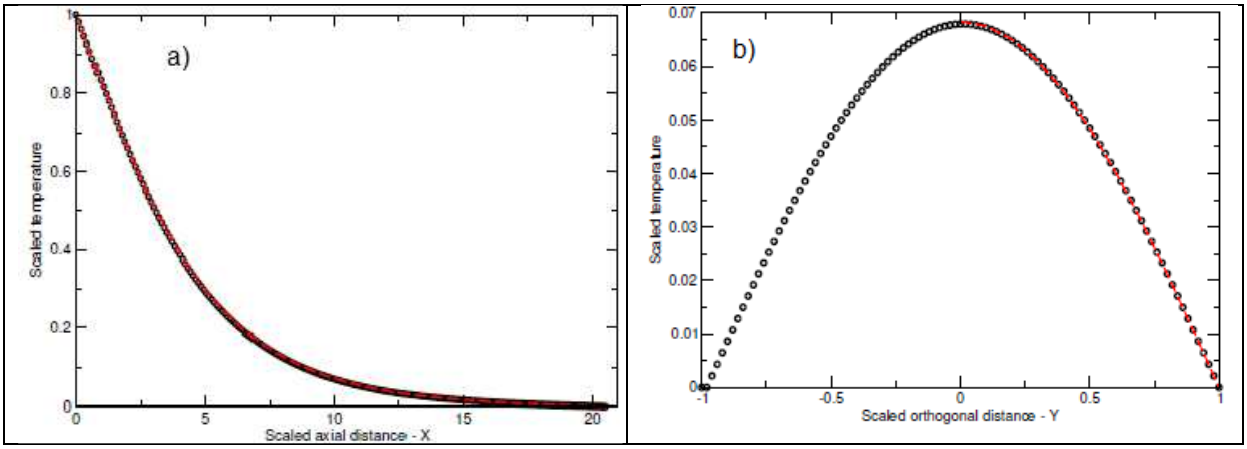

Figure 3: Temperature profile in a 2D Brinkman channel for Peclet number of 0.194 (n_s = 0.4). a) Along the centre-line, parallel to the pressure gradient direction. b) Orthogonal to the centre-line at X = 0.35. Black circles are gray-scale LB result while red-dashed lines are results from finite-difference solution.

5 APPLICATION TO REAL SAMPLES

We have so far validated the gray-scale LB model for single phase flow, multiphase immiscible flow and a coupled fluid flow and temperature model. We would now like to demonstrate the developed models on real world, physical samples. To do this we apply the gray-scale model we have just outlined to digital sample of tight sandstones which consists of quartz, albite, calcite and pyrite obtained from the Yaodian area of Yan'an in Erdors Basin, China. The 3D microscopic distribution of mineral phases in the sample is generated with the DCM software [5]. Each voxel represents a size of 3.7 × 3.7 × 3.7 μm^3 and the total size of the domain we apply the LB method to is 100 × 100 × 120 voxels.

In the sample pyrite, quartz and albite are not permeable. Fluid can flow through the void and the partially permeable calcite. The resistivity to fluid flow of the calcite is not known precisely and so we assume it is proportional to the solid calcite fraction in a voxel. The proportionality constant is denoted n_s^c and can vary from zero (no resistivity) up to one (complete resistivity to fluid flow). Then the bounce-back fraction for a given voxel is given by $n_s = 1 - v_o - n_s^c v_c$, where v_o and v_c denote the volume fractions of void and calcite in a particular voxel respectively.

5.1 Single phase flow

Figure 4 shows the voids (dark blue) and semi-permeable calcite (lighter blue to white) regions in the sample. The solid regions (quartz, albite, pyrite) have been made transparent so as to make the void and calcite regions more easily visible. For this case we use

a n_s^c value of 0.2 which leads to a porosity in the sample of 0.11. To drive the fluid flow a body force of 6.8×10^{-7} in the positive z direction of the sample.

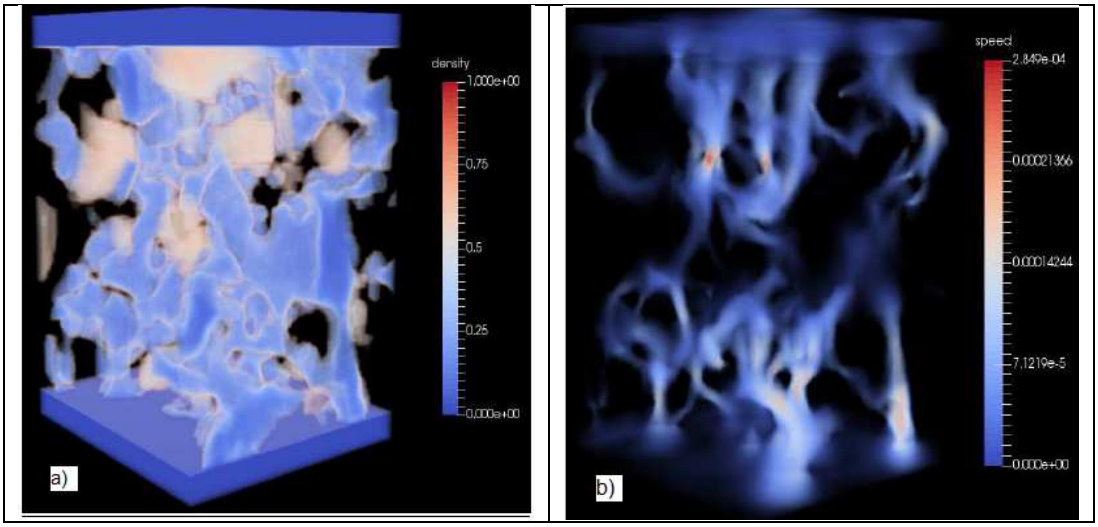

Figure 4: Tight sandstone sample on which we performed the gray-scale LB calculation. a) Distribution of voids (blue) in gray-scale sample. b) Velocity field.

The steady state flow field for the sample is shown in Fig. 4b. One can clearly see lighter coloured flow-paths which align generally with the long (z-axis) of the sample which is primarily due to the body-force in the z direction, but also may indicate a degree of anisotropy in the underlying rock micro-structure. The maximum speed in the sample is approximately 2.8×10^{-4} and is achieved in a few regions (e.g. in the middle of the sample). Overall the speed of the fluid is quite small and reflects the fact that the medium has very low porosity and thus should be quite impermeable. To calculate the sample's permeability, k, we can use the following equation

$$k = \frac{\nu}{G}\langle u \rangle \quad , \qquad (16)$$

where u is the superficial velocity (i.e in the direction of the body force, G) and the angular brackets represent a statistical average over the whole sample. Using this equation we estimate the permeability of the sample is 5.703×10^{-14} m^2 or 57.03 mD. This relatively low permeability reflects a low convective fluid flow.

5.2 Multi-phase immiscible flow

To demonstrate multiphase flow on the rock sample of Fig, 4a we initially placed a reservoir of the invading phase at the inlet (bottom end) and the rock sample is filled with the defending phase (with periodic boundary conditions on all faces). The immiscible fluids are driven through the sample with the same body force (as for single phase flow). In this case there is no (wetting or non-wetting type) interaction of the fluids with the solid matrix, although this can be readily incorporated into the model [6].

Figure 5a shows the flow pattern at breakthrough of the invading phase. In this

complex three-dimensional media, it is difficult to get a full idea of the flow a two-dimensional snap-shot. However, they do show preferential fingering of the invading phase, following paths of least (fluid) resistance. We also calculate the permeability at various times (invading fluid volume fraction) during the flood and this is given in Fig. 5b. For three dimensional flow, both phases can simultaneously have non-zero relative permeability, while in two-dimensions this is generally not possible, i.e. as soon as the invading phase breaks through the defending phase gets cut-off.

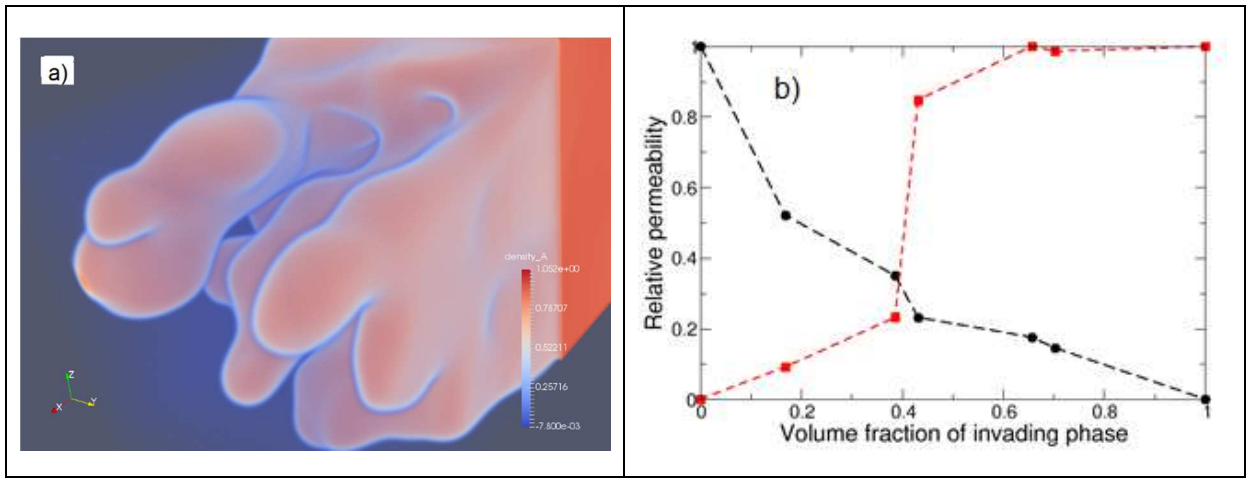

Figure 5 Two phase immiscible flow through the gray-scale tight sandstone sample of Fig. 4a. a) Invading phase (redish-orange colour) at breakthrough. b) Relative permeability curves for invading phase (red) and defending phase (black). The symbols correspond to the LB simulation, while the dashed-lines are only for the eye.

5.3 Coupled temperature and fluid flow

The temperature field for the same rock sample was simulated with two different thermal diffusivities of 1/6 and 1/30. The first diffusivity of 1/6 coupled with the low velocity field magnitude results in a low Peclet number flow. As a result the calculated temperature (Fig. 6a) is quite uniform with a creamy/white shading. As soon as one moves away from the inlet (where the temperature is 1.75) the temperature diminishes rapidly to one. As the solid regions in the sample have an imposed (boundary) temperature of one, the temperature in the adjacent semi-permeable regions is also close to one and the flow field has little effect on the temperature. Thus we are in the diffusion dominated regime for this flow.

For the smaller diffusivity of 1/30 the temperature field shows much more variability with orange/redish colours dispersed throughout the sample. These regions correspond to the higher fluid flow regions (and also the void regions) of the sample. Hence fluid convection now transports the temperature field through the sample.

6 CONCLUSION

We have presented a LB model to treat digital samples where voxels can have a continuum of values between zero and one, which we call a gray-scale model. The model has been developed for single phase flow, multiphase flow and coupled temperature and fluid flow. Each model was firstly validated quantitatively with independent methods and excellent

agreement was obtained. Then each method was applied to a real-world rock sample. The flow fields, fluid displacements and temperature fields were all realistic, which gives us confidence in future applications of this technique.

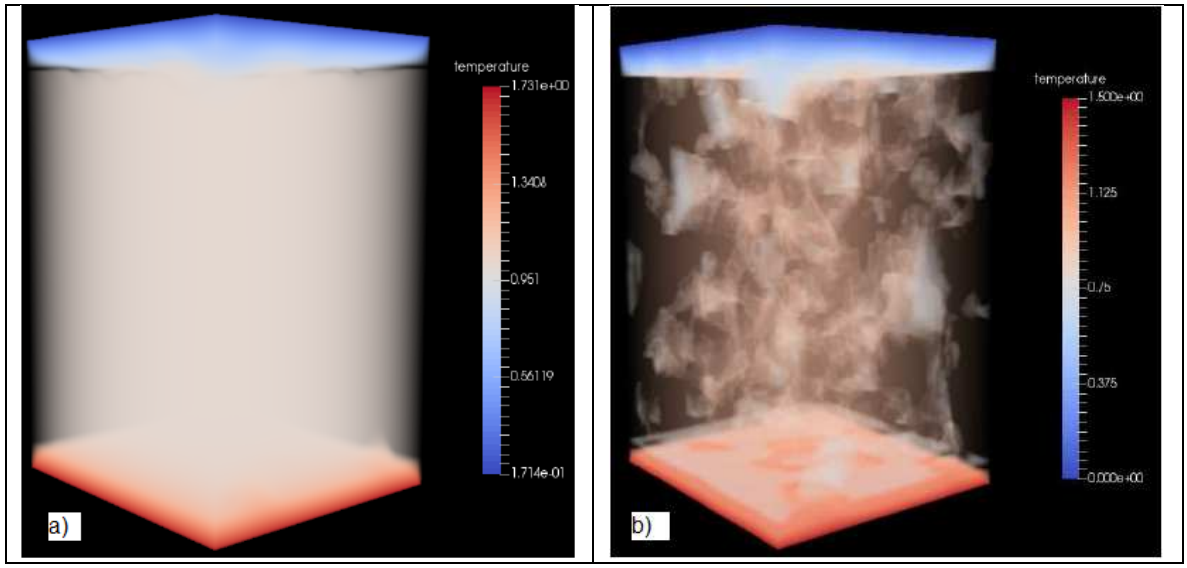

Figure 6: Temperature field for the tight sandstone sample shown in Fig. 4a. a) For a thermal diffusivity of 1/6 which gives a diffusive dominated temperature distribution and b) for a thermal diffusivity of 1/30 which gives a convective dominated temperature distribution.

REFERENCES

[1] Succi, S. *The lattice Boltzmann equation for fluid mechanics and beyond*. Oxford Science, (2001).

[2] Chen, S. and Doolen, G.D. Lattice Boltzmann method for fluid flows. *Annu. Rev. Fluid Mech.* (1998) **30**:329-364.

[3] Walsh, S.D.C., Burwinkle, H. and Saar, M.O. A new partial bounce-back LB method for fluid flow through heterogeneous porous media, *Comp. Geosci*., (2009) **35**: 1186-1193.

[4] Liu, R.R., Yang, Y.S., Pereira, G.G., Clennell, M.B., Taylor, J.A. and Pan, K. Lattice Boltzmann modelling of permeability of porous materials with partially percolating voxels, *Phys. Rev. E*, (2014) **90**: 03301(1-10).

[5] Li, R.R. Chu, C. Yang, Y.S. and Pereira, G.G. CSIRO Data Access Portal (2014). doi: 10.4225/08/53F6E72A0D35E.

[6] Pereira, G.G. A multiphase single relaxation lattice Boltzmann model for heterogeneous porous media, *Appl. Math. Modell.*, (2017) **44**: 160-174.

[7] Shan, X. and Chen, H. Lattice Boltzmann model for simulating multiple phases and components, *Phys. Rev. E*, (1993) **47**:1815–1819.

[8] Shan, X. Simulation of Rayleigh-Bernard convection using a lattice Boltzmann method, *Phys. Rev. E*, (1997) **55**: 2780-2788.

[9] Pereira, G.G., Wu, B. and Ahmed, S. Gray-scale temperature and flow lattice Boltzmann model, submitted to *Comp. Geosci.*, (2017).